Supplementary Information

Achieving selective synthesis of N-benzylformamide via one-step electrocatalytic C-N coupling of CO_2 and benzylamine

*Xiaoqian Gao, Chufan Li, Jingyan Liu, Shaohan Xu, Kuang Chen, and Guohua Zhao**

School of Chemical Science and Engineering, Department of Thoracic Surgery,

Shanghai Tongji Hospital, Tongji University, Shanghai 200092, P.R. China

* Corresponding author.

Email: g.zhao@tongji.edu.cn (G. Zhao)

Experimental section

Electrochemical measurements

The linear sweep voltammetry (LSV) curves were conducted with the scan rate of 50 mV s^{-1} in the following solutions: CO_2-saturated 0.1 M $KHCO_3$, Ar-saturated 0.1 M $KHCO_3$, CO_2-saturated 0.1 M $KHCO_3$ containing 0.1 M benzylamine, Ar-saturated 0.1 M $KHCO_3$ containing 0.1 M benzylamine. Double-layer capacitance (Cdl) measurements were conducted to calculate the electrochemically active surface area (ECSA), with cyclic voltammetry (CV) tests carried out at various scan rates (10 to 100 mV s^{-1}) in a 0.1 M $KHCO_3$ solution.

In situ infrared spectroscopy measurements

In situ electrochemical infrared spectroscopy measurements were conducted in external reflection mode using a custom quartz four-neck cell equipped with a CaF_2 optical window. The catalyst ink was prepared by dispersing 4 mg catalyst in 500 μL of a water/ethanol/Nafion mixture, and 20 μL of the ink was dropped on a glassy carbon working electrode. Pt wire and saturated calomel electrode were employed as the counter and reference electrode, respectively. Measurements were performed in 10 mL of CO_2-saturated 0.1 M $KHCO_3$ containing 0.1 M benzylamine. Spectra were collected on a Nicolet 8700 spectrometer (Thermo Fisher Scientific Inc.) during chronoamperometry and were processed by background subtraction and baseline correction.

In situ Raman measurements

Confocal Raman microscopy (inVia, Renishaw) with a 532 nm laser was used for *in situ* Raman measurements, calibrated against a silicon wafer at 520.5 cm^{-1} beforehand. Tests were conducted in a custom single-chamber Teflon electrolytic cell with a circular quartz window. A catalyst-loaded carbon paper electrode (1 mg cm^{-2}), Pt sheet and saturated calomel electrode acted as working, counter and reference electrodes, respectively. The electrolyte was 5 mL CO_2-saturated 0.1 M $KHCO_3$ with 0.1 M benzylamine, and potentials were controlled via a CHI660 electrochemical workstation.

Online differential electrochemical mass spectrometry (DEMS) measurements

Online DEMS measurements were carried out in a custom cell. CO_2-saturated 0.1 M $KHCO_3$ containing 0.1 M benzylamine was circulated through the cell using a peristaltic pump. The working

electrode was a graphite sheet coated with catalyst. Platinum gauze and saturated calomel were counter electrode and reference electrode, respectively. All measurements included three consecutive potentiostatic cycles to guarantee reproducibility. Gaseous products and reaction intermediates generated during C-N coupling were pumped into a mass spectrometer for detection.

Product quantitation

The gaseous products were monitored online employing a gas chromatography (GC-2014C, Shimadzu, Japan, H_2 and N_2 carrier) equipped with a thermal conductivity detector, a flame ionization detector, and a methanizer. The aqueous products (formate, N- benzylformamide, and other byproducts) were analyzed by ^{1}H NMR (Bruker AVANCE-HD 600 MHz). Typically, 500 μL of final catholyte was mixed with 50 μL mixture solution of D_2O and DMSO (4 μL DMSO was added into 5 g of D_2O). FE values of the products were calculated with the equation:

$$FE\ (\%) = \frac{2 * n * F}{Q} * 100$$

where 2 is electron transfer number, n denotes the moles of products, F is Faradaic constant (96485 C mol^{-1}), Q represents the total charge accumulated during reaction.

Characterization

Transmission electron microscopy (TEM) and high-resolution TEM (HR-TEM) images were obtained by JEM-2100 (200 kV, JEOL, Japan). The scanning electron microscopy (SEM) was conducted by JSM-7900F (5 kV, JEOL, Japan). High-angle annular dark-field scanning transmission electron microscopy (HAADF-STEM) images were obtained on a 300 kV FEI Titan G2 80-300 microscope with a probe corrector. The inductively coupled plasma mass spectrometry (ICP-MS, Agilent 7800, U.S.A.) was used to determine the content of Sn element in catalysts. X-ray diffraction measurements were performed on Bruker D8 Focus diffractometer equipped with a Cu radiation source (λ = 1.540598 nm). The surface coordination analysis of catalyst was performed on an X-ray photoelectron spectroscopy (XPS, Thermo Scientific, U.S.A.) using Al Kα target as the excitation source. All XPS binding energies were calibrated against the C 1s reference peak at 284.8 eV.

Supplementary Figures and Tables

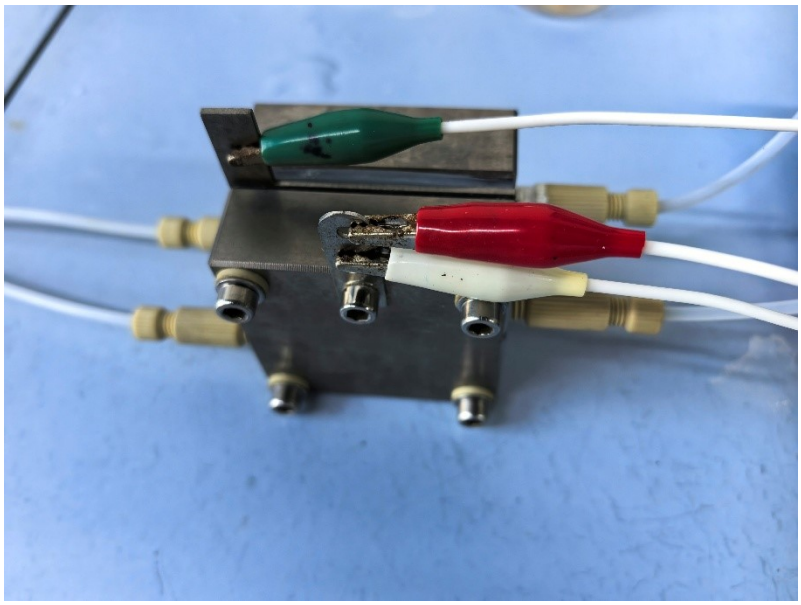

Fig. S1 The photo of applied MEA reactor.

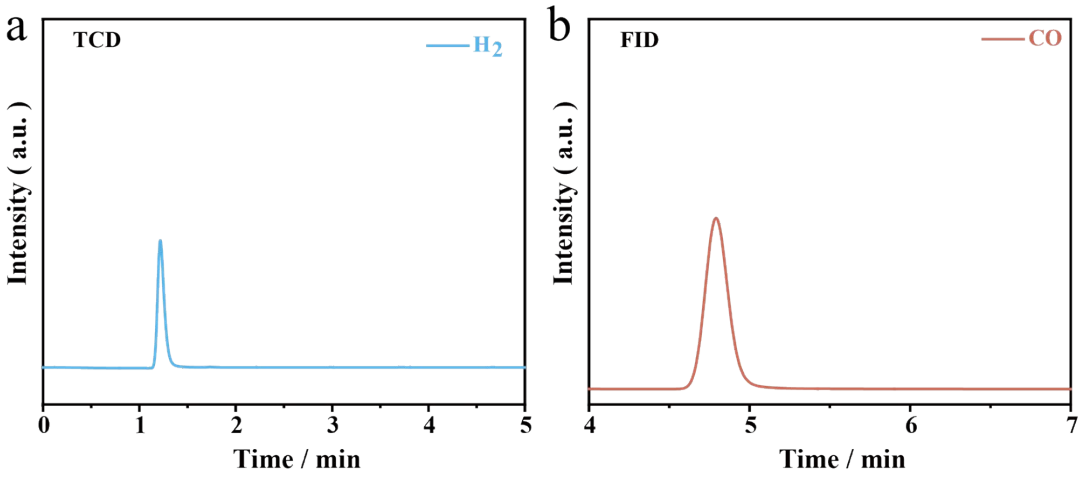

Fig. S2 The detection for gas products of (a) H_2 in TCD and (b) CO in FID via gas chromatography.

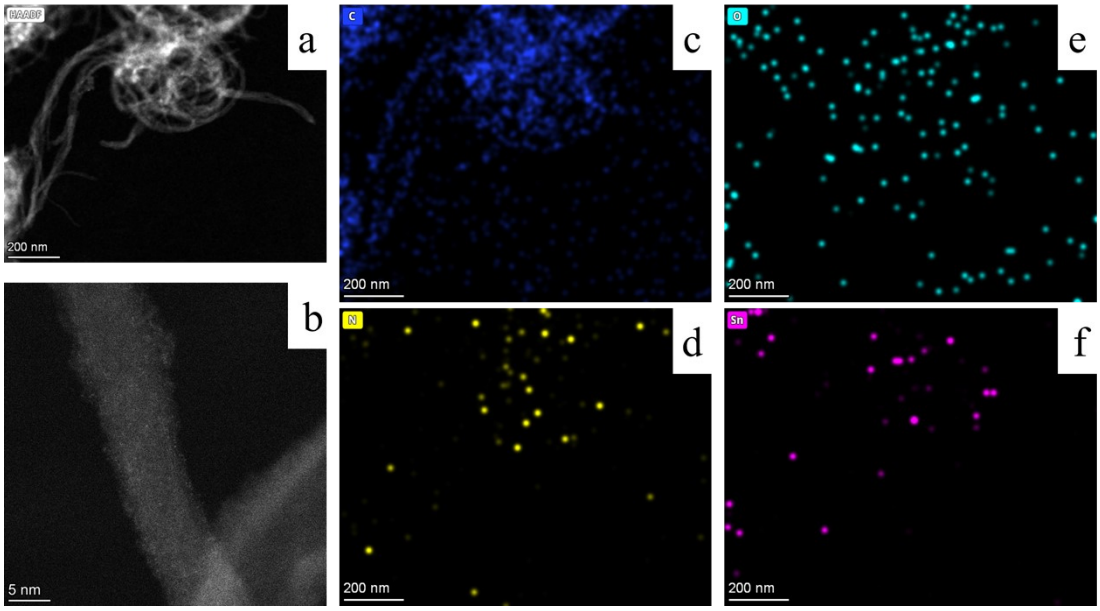

Fig. S3 HAADF-STEM images and EDS mapping of C-O-SnPc-1 catalyst.

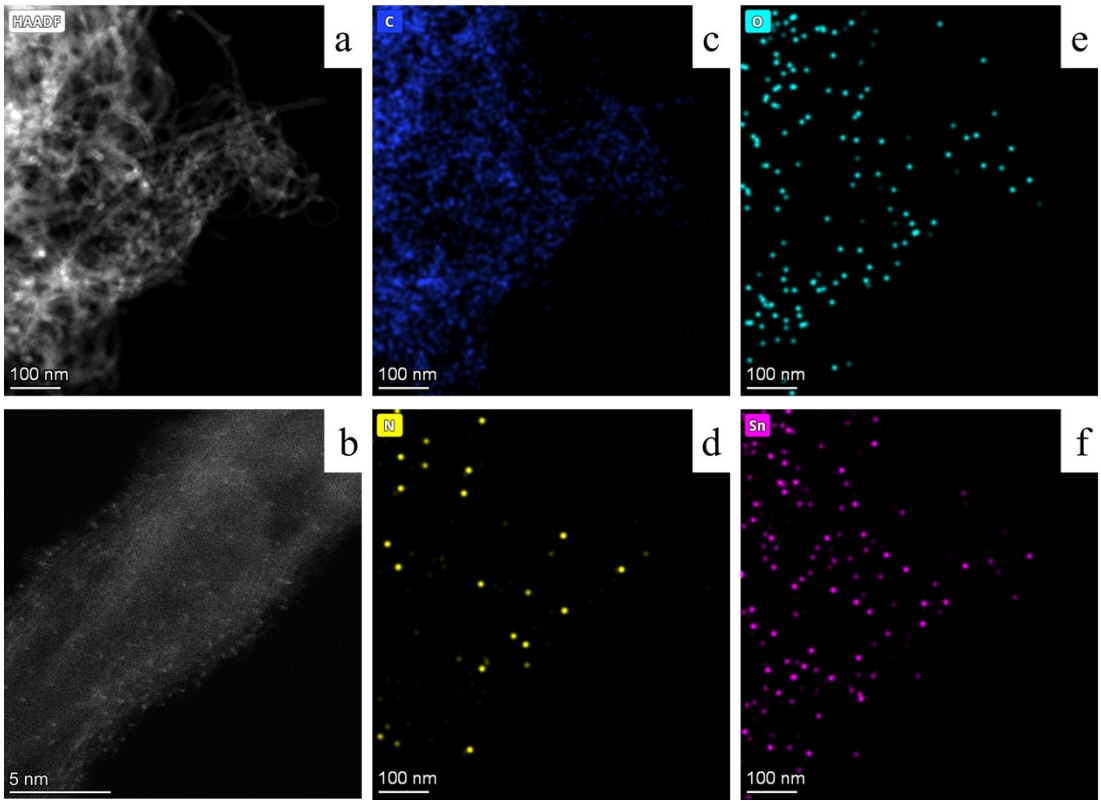

Fig. S4 HAADF-STEM images and EDS mapping of C-O-SnPc-2 catalyst.

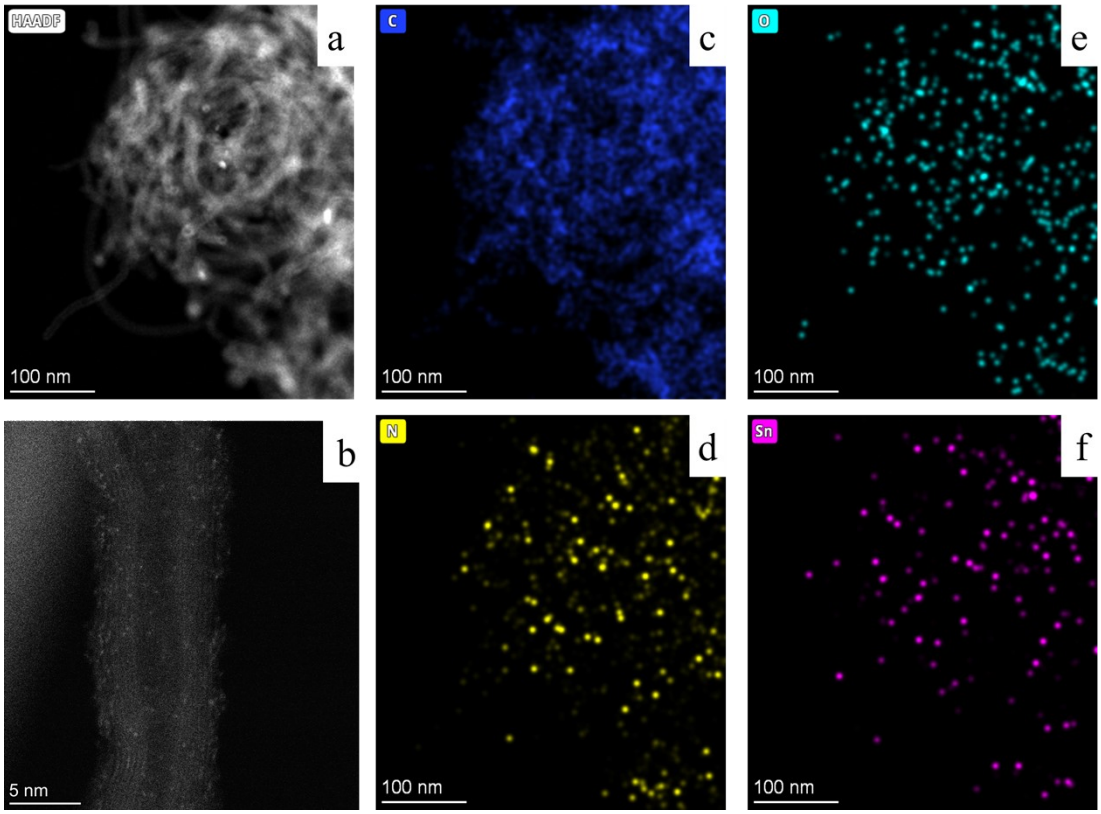

Fig. S5 HAADF-STEM images and EDS mapping of C-O-SnPc-3 catalyst.

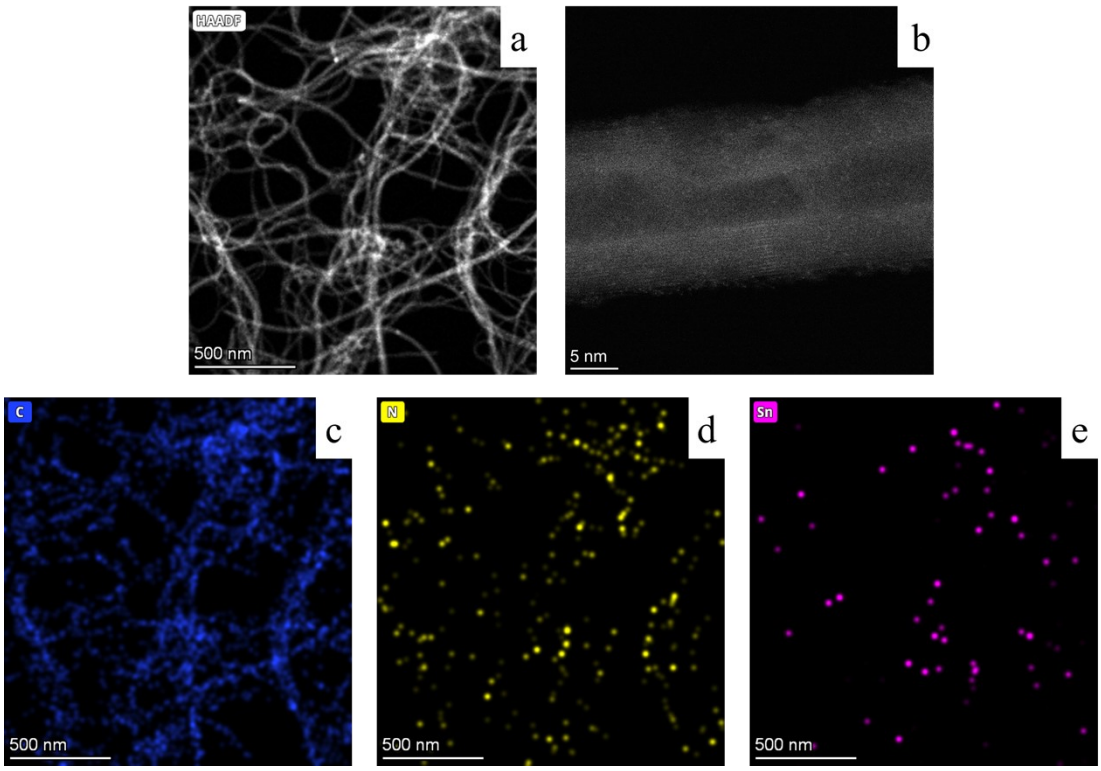

Fig. S6 HAADF-STEM images and EDS mapping of SnPc/CNT catalyst.

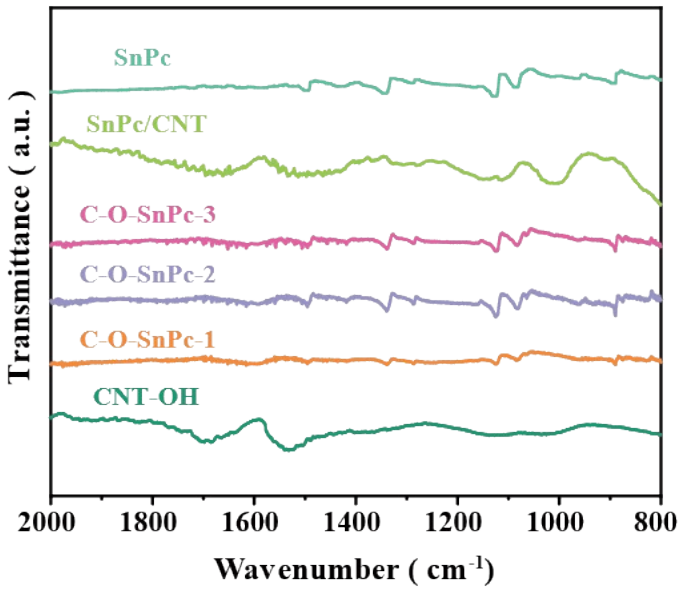

Fig. S7 FT-IR spectra of CNT-OH, C-O-SnPc-1, C-O-SnPc-2, C-O-SnPc-3, SnPc/CNT, and SnPc catalysts.

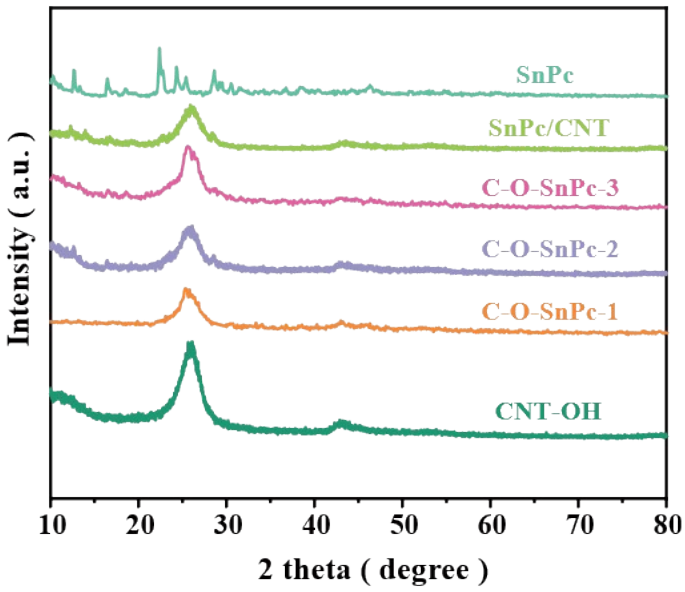

Fig. S8 XRD patterns of CNT-OH, C-O-SnPc-1, C-O-SnPc-2, C-O-SnPc-3, SnPc/CNT, and SnPc catalysts.

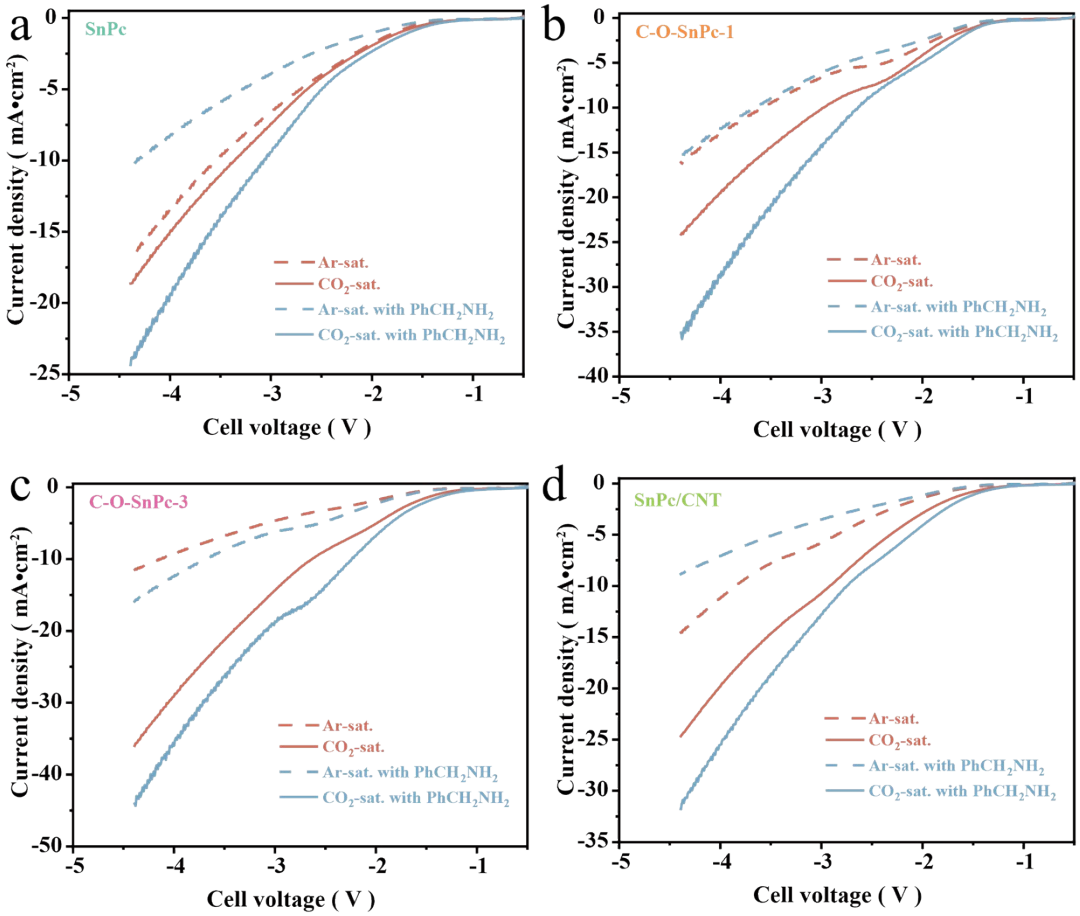

Fig. S9 LSV curves obtained in four conditions (Ar-saturated 0.1 M $KHCO_3$, CO_2-saturated 0.1 M $KHCO_3$, Ar-saturated 0.1 M $KHCO_3$ containing 0.1 M benzylamine ($PhCH_2NH_2$), and CO_2-saturated 0.1 M $KHCO_3$ containing 0.1 M $PhCH_2NH_2$) of (a) SnPc, (b) C-O-SnPc-1, (c) C-O-SnPc-3, and (d) SnPc/CNT catalysts.

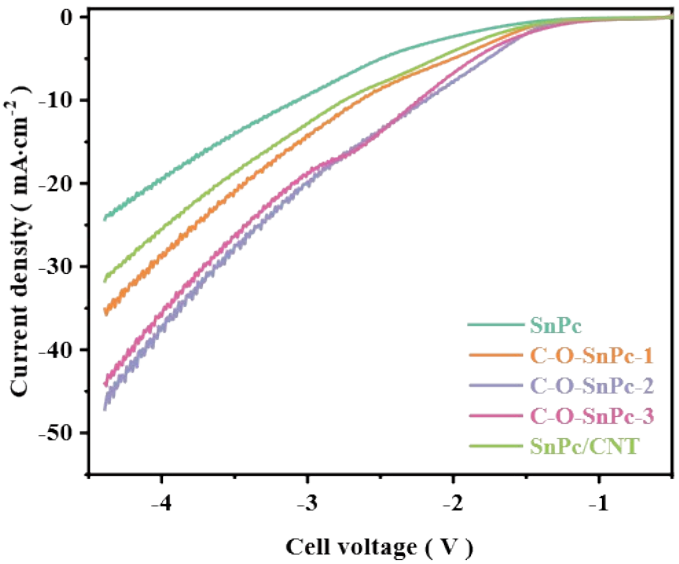

Fig. S10 LSV curves of catalysts (SnPc, C-O-SnPc-x, and SnPc/CNT) under C-N coupling (CO_2-saturated 0.1 M $KHCO_3$ containing 0.1 M benzylamine).

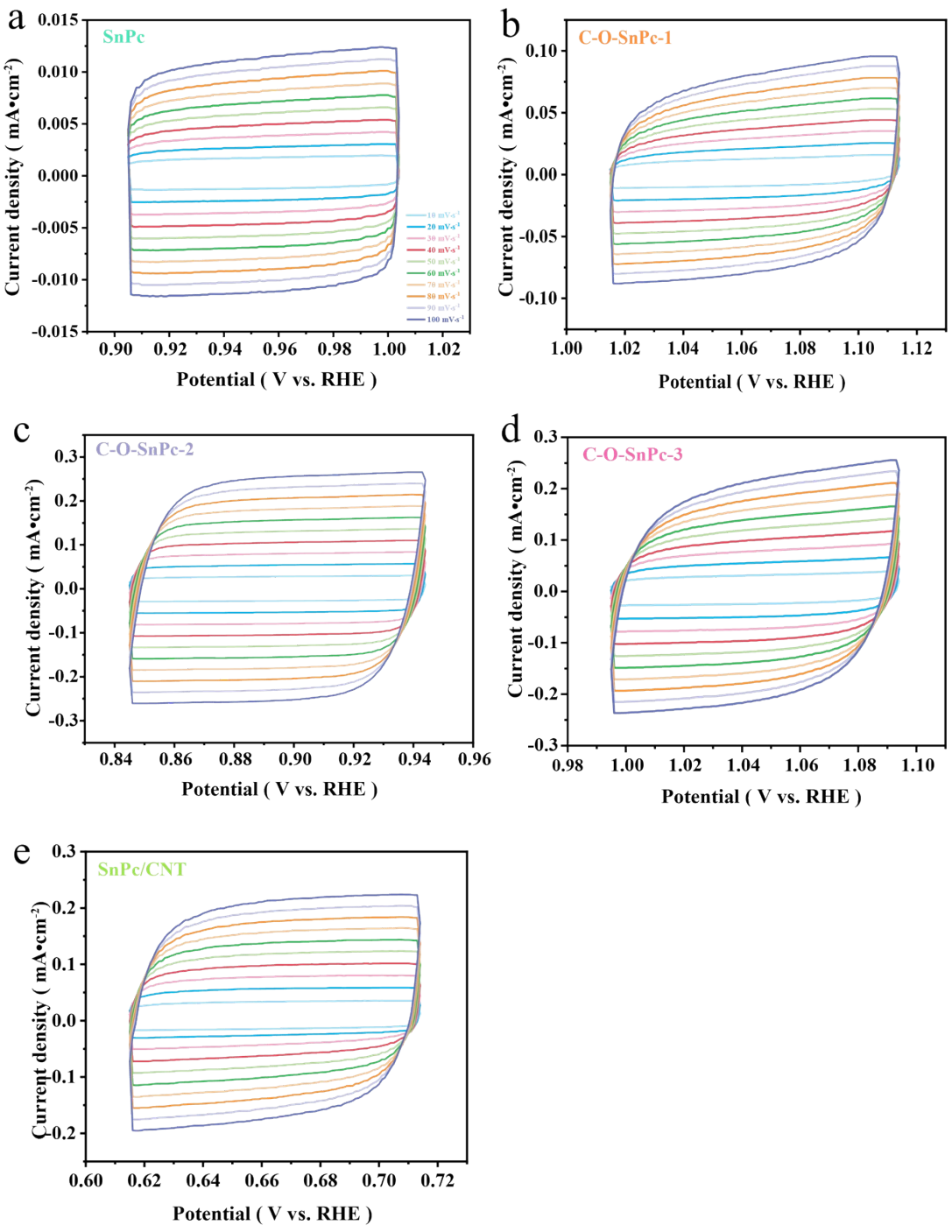

Fig. S11 CV curves conducted under OCP of (a) SnPc, (b) C-O-SnPc-1, (c) C-O-SnPc-2, (d) C-O-SnPc-3, and (e) SnPc/CNT catalysts at the scan rates of 10 – 100 mV s^{-1}.

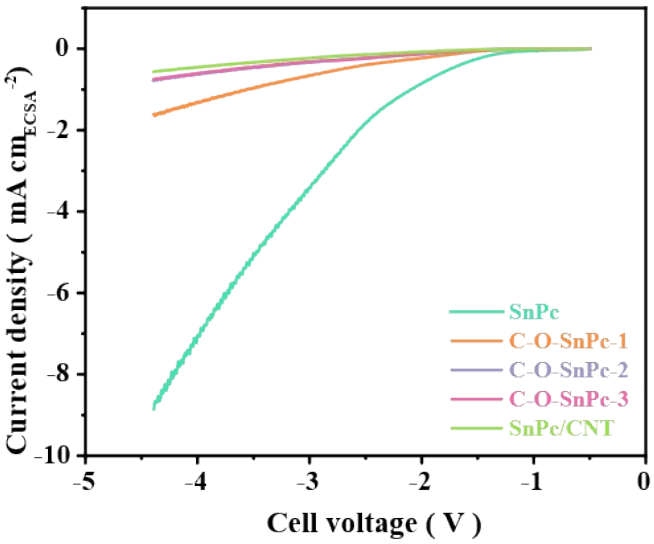

Fig. S12 LSV curves of catalysts (SnPc, C-O-SnPc-x, and SnPc/CNT) under C-N coupling when the current densities were normalized by ECSA.

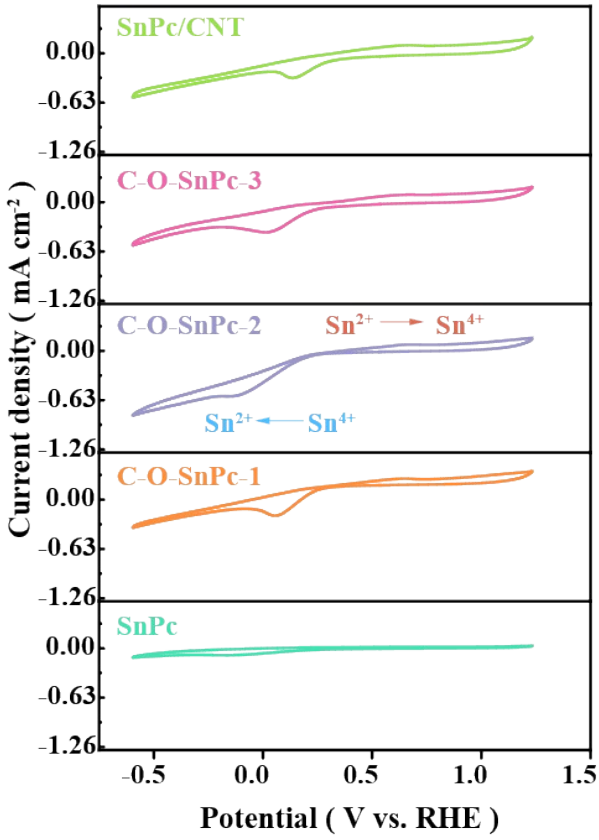

Fig.S13 CV curves of catalysts in Ar-saturated 0.1 M $KHCO_3$.

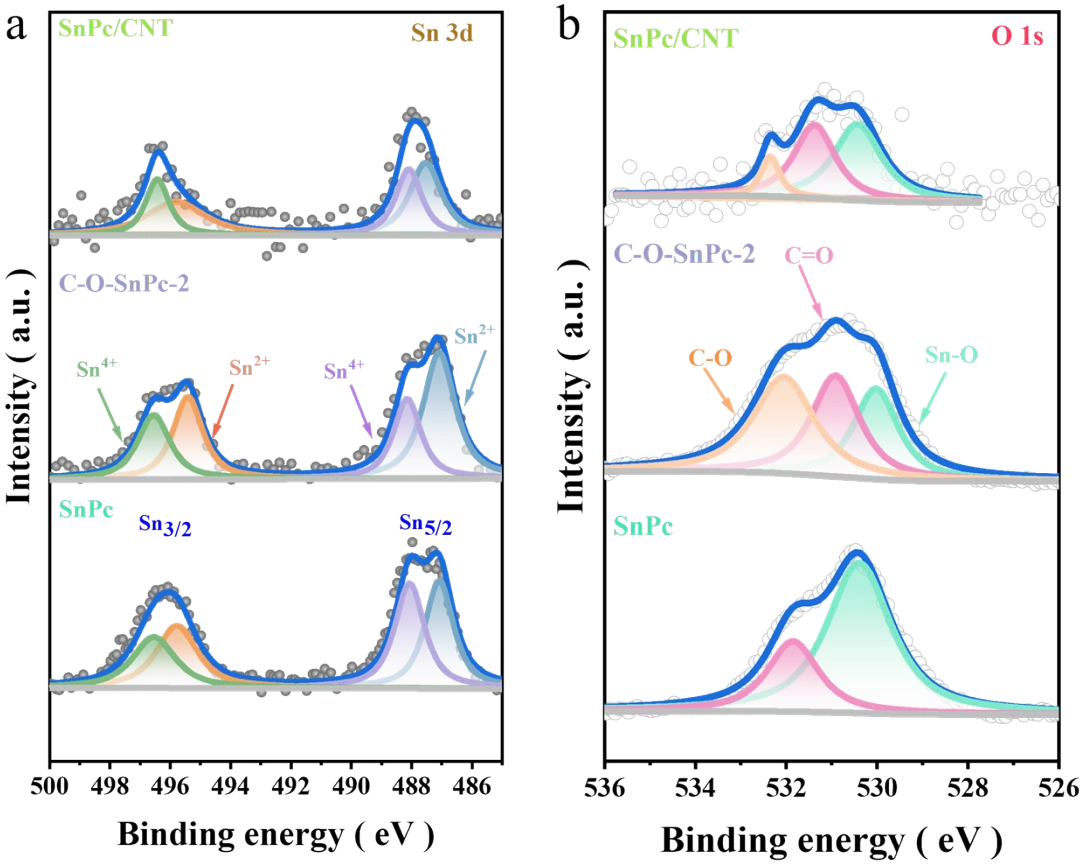

Fig. S14 (a) Sn 3d and (b) O 1s XPS spectra of SnPc, C-O-SnPc-2, and SnPc/CNT catalysts before electrolysis.

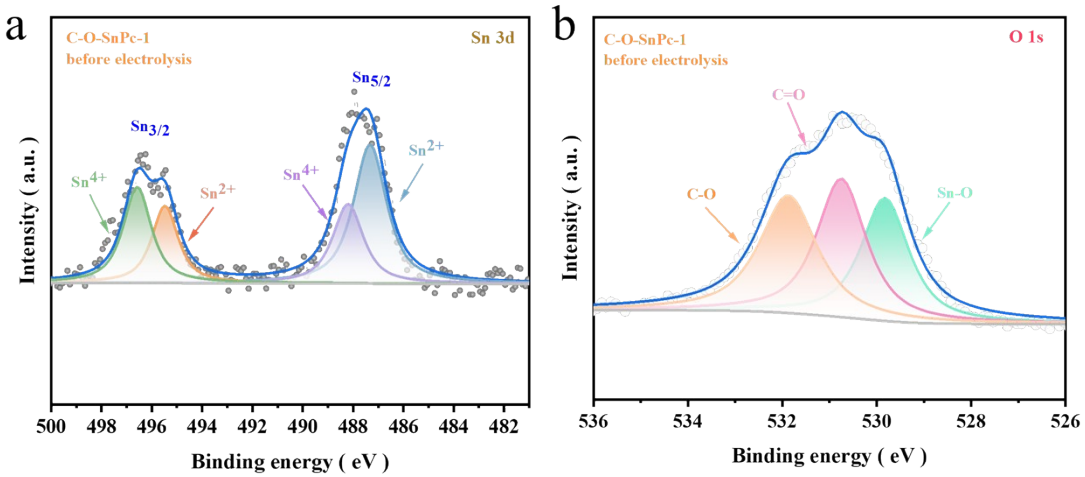

Fig. S15 (a) Sn 3d and (b) O 1s XPS spectra of C-O-SnPc-1 catalyst before electrolysis.

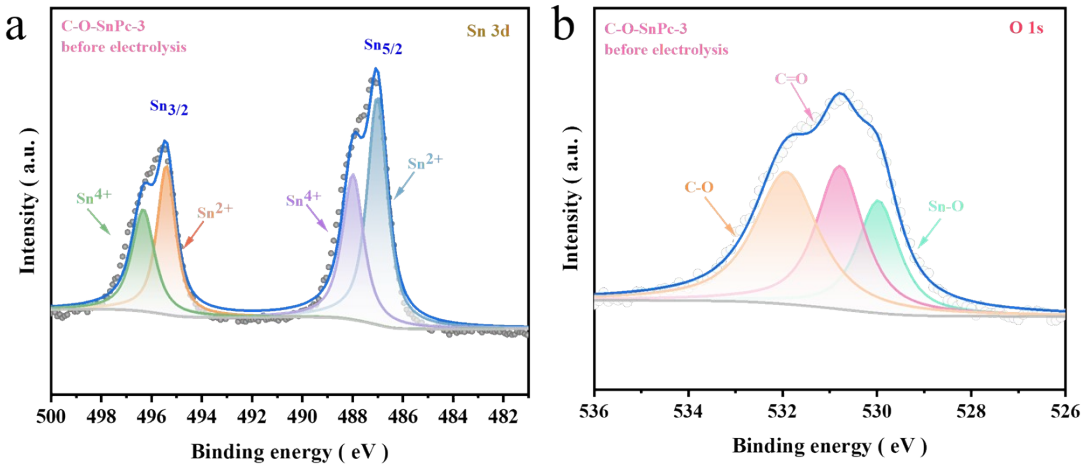

Fig. S16 (a) Sn 3d and (b) O 1s XPS spectra of C-O-SnPc-3 catalyst before electrolysis.

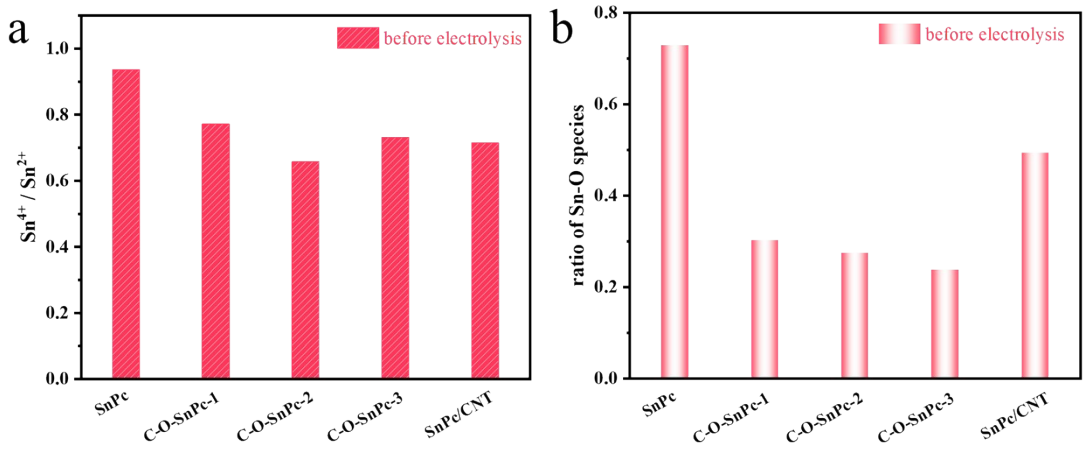

Fig. S17 (a) Sn^{4+}/Sn^{2+} ratio and (b) the ratio of Sn-O species calculated from XPS spectra of SnPc, C-O-SnPc-1, C-O-SnPc-2, C-O-SnPc-3, and SnPc/CNT catalysts before electrolysis.

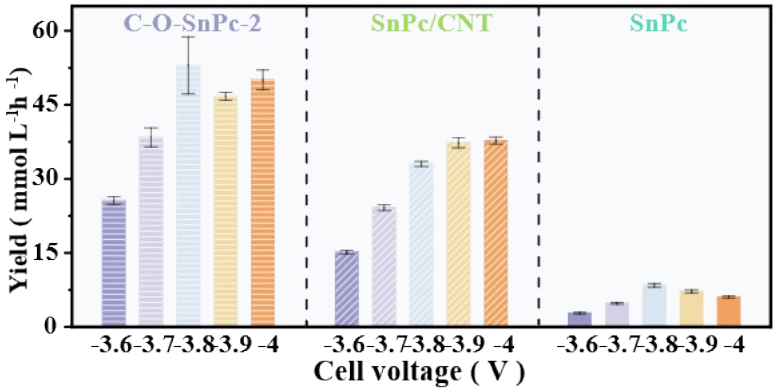

Fig. S18 Yields for N-benzylformamide of C-O-SnPc-2, SnPc/CNT, and SnPc under different applied cell voltage.

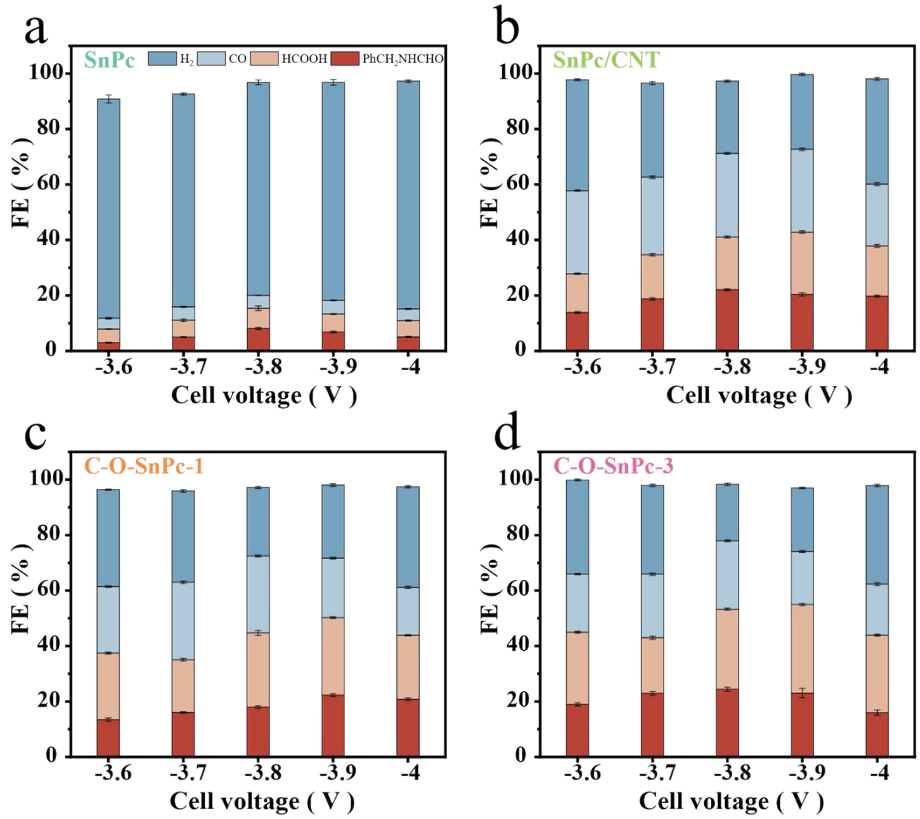

Fig. S19 FEs for gaseous and liquid products of (a) SnPc, (b) SnPc/CNT, (c) C-O-SnPc-1, and (d) C-O-SnPc-3 under different applied cell voltage.

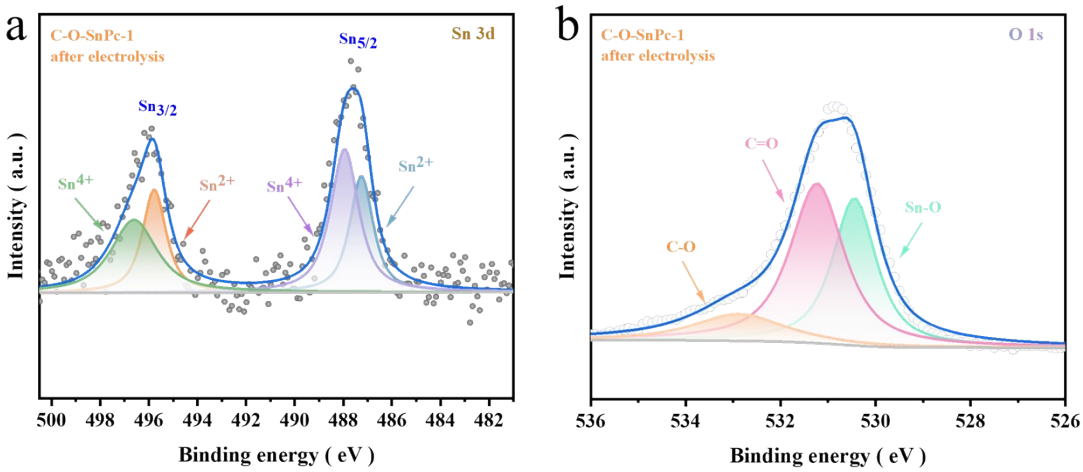

Fig. S20 (a) Sn 3d and (b) O 1s XPS spectra of C-O-SnPc-1 catalyst after electrolysis.

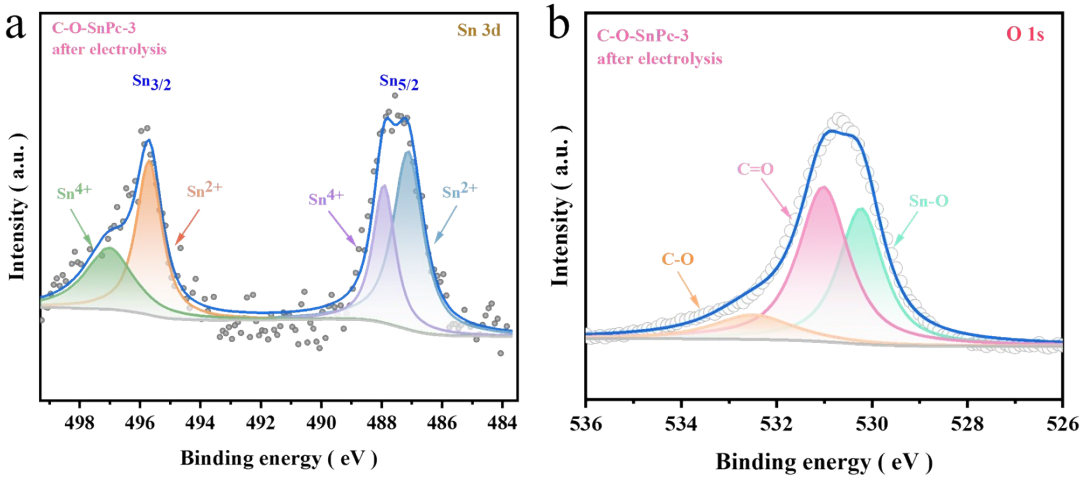

Fig. S21 (a) Sn 3d and (b) O 1s XPS spectra of C-O-SnPc-3 catalyst after electrolysis.

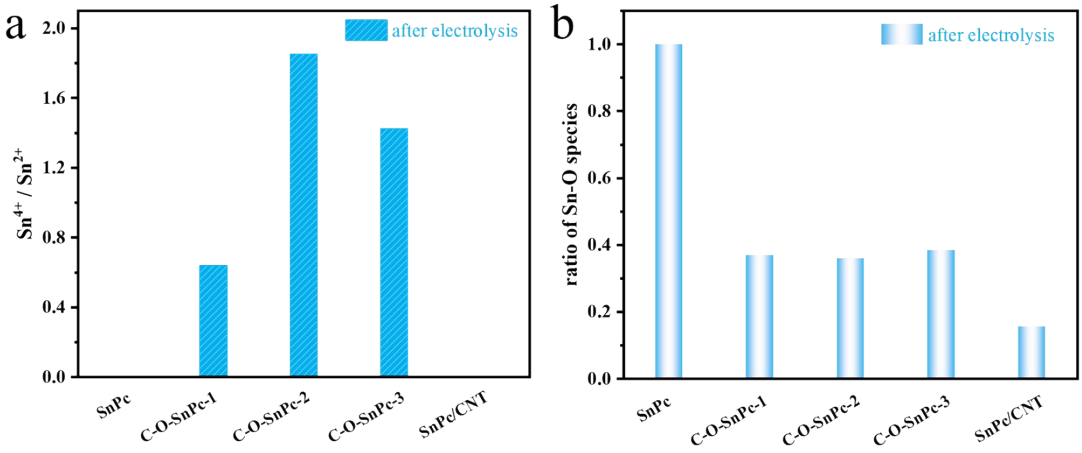

Fig. S22 (a) Sn^{4+}/Sn^{2+} ratio and (b) the ratio of Sn-O species calculated from XPS spectra of SnPc, C-O-SnPc-1, C-O-SnPc-2, C-O-SnPc-3, and SnPc/CNT catalysts after electrolysis.

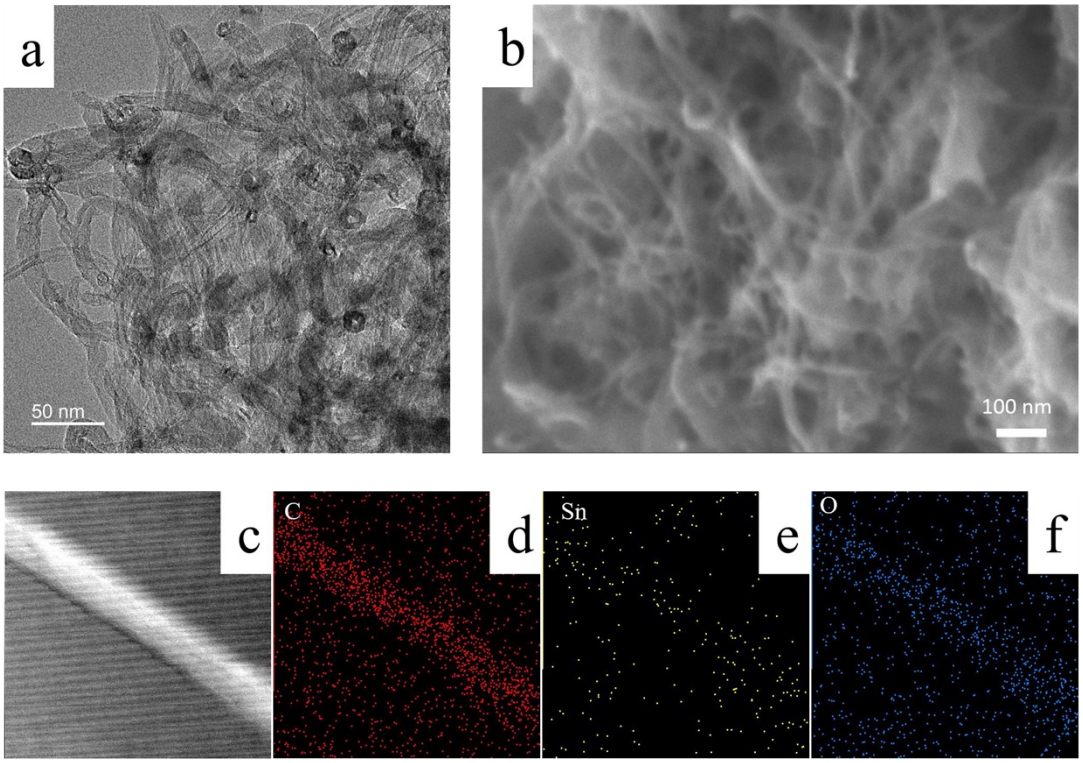

Fig. S23 (a) TEM image, (b) SEM image and (c−f) EDS mapping of C-O-SnPc-2 catalyst after electrolysis.

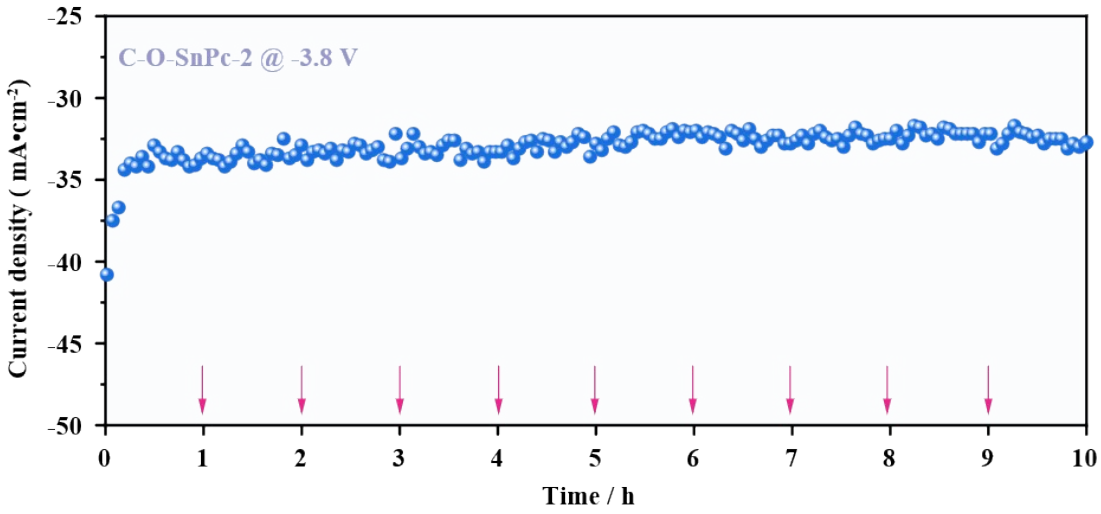

Fig. S24 Current density in long-term stability of CO_2 and benzylamine C-N coupling on the C-O-SnPc-2 catalyst at a cell voltage of –3.8 V in MEA cell. The vertical arrow denotes the time for electrolyte refreshment.

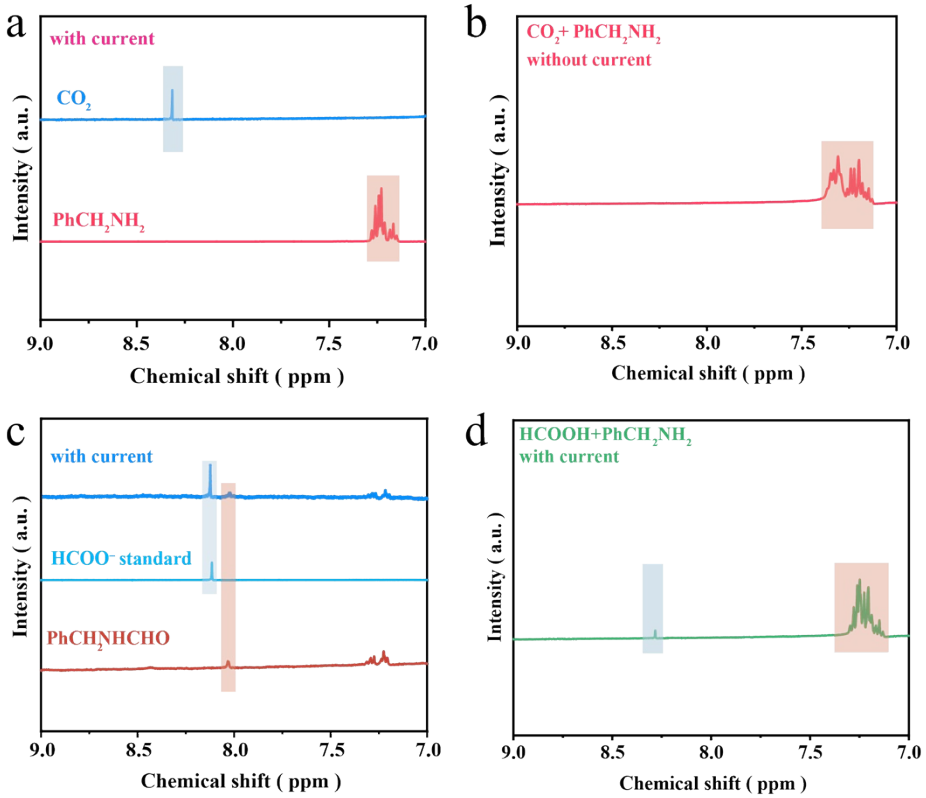

Fig. S25 (a) ^{1}H NMR spectra of C-O-SnPc-2 under applied potential when only CO_2 or benzylamine ($PhCH_2NH_2$) was used as the reactant. (b) ^{1}H NMR spectra of C-O-SnPc-2 without current when CO_2 and $PhCH_2NH_2$ was used. (c) ^{1}H NMR spectra of standard references (N-benzylformamide ($PhCH_2NHCHO$) and $HCOO^-$) and C-N coupling under applied potential. (d) ^{1}H NMR spectra of C-O-SnPc-2 with current when HCOOH and $PhCH_2NH_2$ was used.

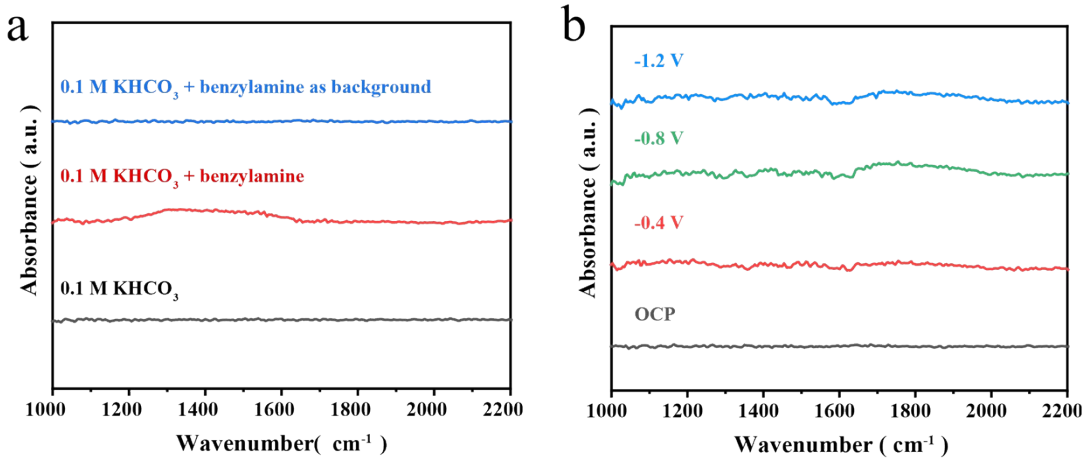

Fig. S26 (a) FT-IR spectra of different electrolyte in different mode. (b) In situ FT-IR spectra of Ar-saturated electrolyte (0.1 M $KHCO_3$ + 0.1 M benzylamine) under applied potentials.

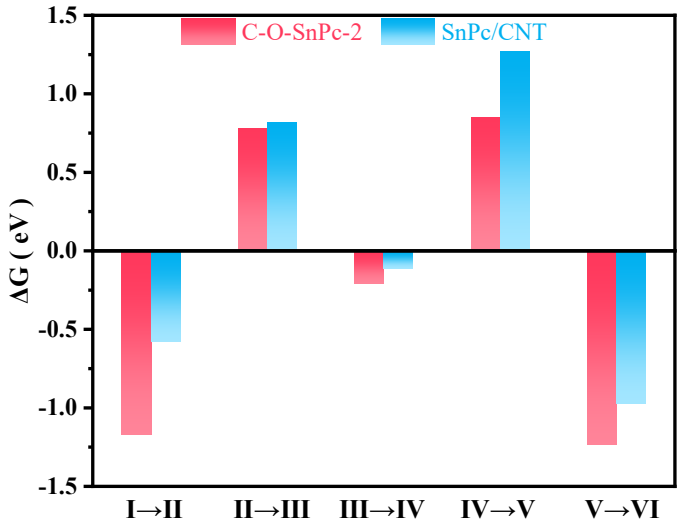

Fig. S27 Calculated ΔG for steps during C-N coupling over C-O-SnPc-2 and SnPc/CNT catalysts.

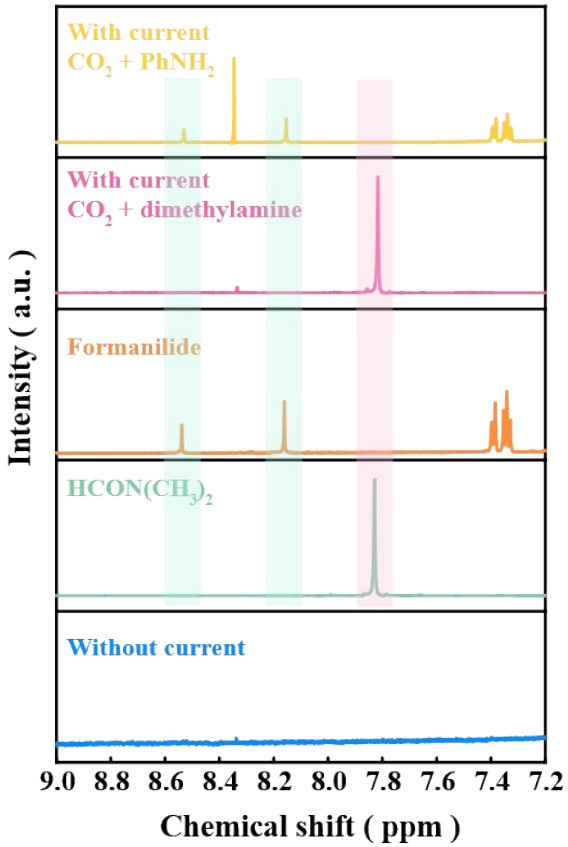

Fig. S28 ^{1}H NMR spectra of pure $HCON(CH_3)_2$ and pure formanilide. ^{1}H NMR spectra of C-O-SnPc-2 in electrolyte without current, under –3.8 V when CO_2 and dimethylamine (or $PhNH_2$) was used as the reactant.

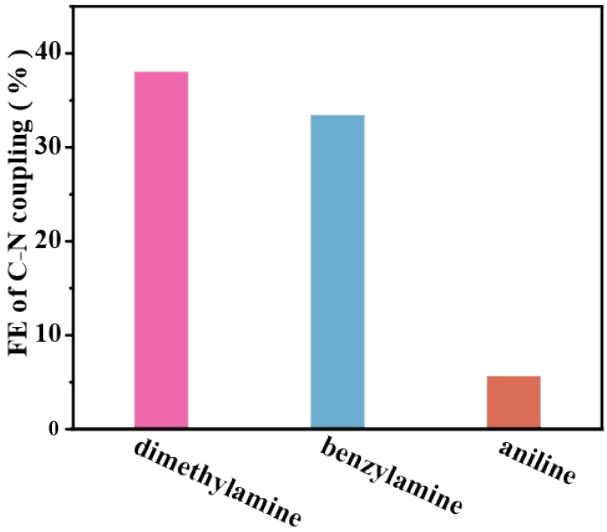

Fig. S29 FEs of C-N coupling in the substrate tests when dimethylamine, benzylamine and aniline were used as the reactant, respectively.

Table S1. Sn content of catalysts determined by EDS mapping and ICP-MS

Sample	Sn (at%) by EDS	Sn (wt%) by ICP-MS
SnPc	1.34	12.4
C-O-SnPc-1	0.09	2.8
C-O-SnPc-2	0.18	3.9
C-O-SnPc-3	0.24	4.5
SnPc/CNT	0.15	3.7

Table S2. The calculated Cdl and ECSA values for catalysts according to CV curves

Sample	Cdl ($mF \cdot cm^{-2}$)	ECSA (cm^{-2})
SnPc	0.11	2.75
C-O-SnPc-1	0.87	21.75
C-O-SnPc-2	2.58	64.5
C-O-SnPc-3	2.35	58.75
SnPc/CNT	2.25	56.25

Table S3. Summary of FEs for C-N coupling using CO_2 and amines as reactants

C source	N source	Product	Catalyst	FE (%)	Ref
CO_2		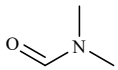	InN_3	22.4	[20]
	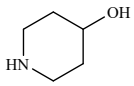	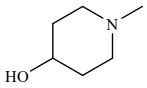	$CuO/NiAl_2O_4$	29.3	[23]
	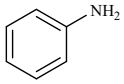	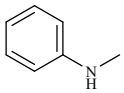	$CuO/NiAl_2O_4$	8.8	[23]
			$CuO/NiAl_2O_4$	13.6	[23]
			CoPc/CNT	1	[21]
			CoPc/CNT	3.4	[21]
	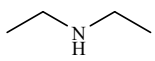	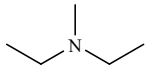	CoPc/CNT	2.9	[21]
			CoPc/CNT	7.5	[21]
	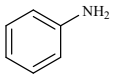	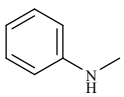	CoPc/CNT	0.6	[21]
		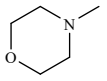	CoPc/CNT	2.5	[21]
	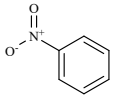	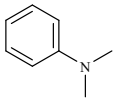	CoN_2O_2-$(OH)_2$	13.5	[5]
	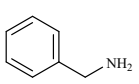	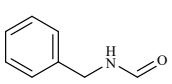	C-O-SnPc	33.4	This work